Rotational Effects on Natural Convection in a Horizontal Cylinder

A numerical computation is carried out to study the interaction of rotation and natural convection inside a finite horizontal cylinder. The natural convection is due to differential heating on the two ends, while the rotation is along the axis of the horizontal cylinder. The aspect ratio, length of the cylinder to its radius, is 2.0. The Grashof number is fixed at 1.43×10^6 with air as a working fluid. The effect of rotation is examined with Gr/Re^2 from 7.0×10^{-2} to ∞, which covers the range from rotation dominated flow to buoyancy dominated flow. It is found that when rotational speed is relatively small or $Gr/Re^2 \gg 1$, the effect of rotation is to render the spatial heat flux distribution more uniform. As the rotational speed increases, the heat transfer rate distribution on the end surfaces is more homogenous and its level is also reduced. When the rotational speed is sufficiently high ($Gr/Re^2 \ll 1.0$), heat transfer is by conduction only and the whole fluid inside the enclosure rotates as a rigid body. It is shown that there exists a rotation speed range in which one can have both relatively high and uniform heat transfer rates on the end walls.

H. Q. Yang, K. T. Yang
Department of Aerospace and Mechanical Engineering
University of Notre Dame
Notre Dame, IN 46556

J. R. Lloyd
Department of Mechanical Engineering
Michigan State University
East Lansing, MI 48824

Introduction

The study of natural convection inside a horizontal cylinder with differentially-heated ends has an important application in the understanding of crystal growth by chemical vapor transport (Rosenberger, 1979; Ostrach, 1983). The convection which is induced by both thermal and concentration gradients has both positive and negative influences on the crystal growth. For instance, convection augments the transfer rate because the chemical reaction rate is much faster than the diffusion rate, so that the process is diffusion controlled. In this case, convection will speed up the transport process. On the other hand, however, the convection introduces nonuniformity in both mass and heat fluxes on the end surfaces, which will adversely affect the quality of the grown crystal.

The ideal situation is to grow the crystal as fast as possible, at the same time ensuring its chemical uniformity and crystallographic perfection (Solan and Ostrach, 1976). To do so, several approaches have been proposed to control convection so that heat and mass fluxes over the growing crystal are uniform in space and time within prescribed bounds. Methods include using different sizes of ampule, inclining the enclosure with respect to gravity, using both vertical and horizontal thermal gradients and flow stabilizing baffles, enclosing the enclosure in an insulating jacket to reduce the temperature gradient near the growing crystal, changing the temperature difference applied across the two ends with time, etc. A good example is that practiced by Mughal and Ray (1974), in which the cylindrical enclosure (ampule) was inclined and a graphite rod was inserted to eliminate natural convection. Presented in this paper is another approach in which convection is controlled by rotating the cylinder along its axis.

Numerical simulations of natural convection for crystal growth by vapor deposition in ampules has been attempted by Markham and Rosenberger (1983), Ranganathan and Viskanta (1987), and others using two-dimensional rectangular enclosures with both temperature and concentration differences at the two ends. As shown in the experiment by Schiroky and Rosenberger (1984), the flow characteristics in a cylindrical geometry are quite different from the one predicted by a two-dimensional rectangular enclosure. It is observed that the flow is a double helix along both upper and lower halves of the cylinder cavity, and there exists an early initiation of the downward and upward flows in the bulk flow toward the cold and hot ends, respectively. These have also been found in the numerical calculations for a finite cylinder by Smutek et al. (1985) with a higher aspect ratio ($L/R = 10.0$) and moderate Rayleigh numbers ($Ra = 74 - 1.8 \times 10^4$), and by Yang et al. (1988) with a lower aspect ratio ($L/R = 2.0$) and higher Rayleigh numbers ($Ra = 10^4 - 10^7$). It appears that only the cylindrical geometry would

be appropriate to the realistic phenomena of crystal growth by chemical vapor transport.

For combined rotation and natural convection inside cylinders, only a few vertical cylindrical annulus cases have been studied (Hessami et al., 1987; Randriamampiania et al., 1987), in which the gravitational force is considered to be independent of the azimuthal direction so that a two-dimensional problem can be solved with axial symmetry. For the present problem, since natural convection is driven by horizontal temperature gradient and vertical gravity force, and its circulation is along the axis perpendicular to the axis of the cylinder or to the axis of rotation, the interaction of the two effects will be expected to lead to complicated three-dimensional flows. Results of the present study are obtained by finite-difference calculations.

Formulations and Limiting Analysis

Rotational properties can be described in two frames of reference. One is in the inertial frame, and the other is in the rotational frame. In the former, velocities are written relative to the ground so that the governing equations retain the same form as those without rotation, but the nonslip boundary conditions on the wall will result in an azimuthal velocity,

$$v_\theta = R\Omega \quad \text{at } r = R \tag{1}$$

and

$$v_\theta = r\Omega \quad \text{at } z = 0 \text{ and } z = L \tag{2}$$

where the symbols are defined in the nomenclature. For the latter case, however, the velocities are written relative to the rotational frame of reference, which results in additional terms due to the transformation of equations. However, the velocity components are zero on the physical boundaries.

Theoretical analysis can be made easier in the rotational frame of reference, in that the relative importance of the various forces can be directly compared so that a qualitative flow structure can be predicted. The transformation of the equations from an inertial frame to a rotational frame can be made by relating the velocity vectors in the different frames (Hamady, 1987),

$$\boldsymbol{v}_{in} = \boldsymbol{v}_{ro} + \boldsymbol{\omega} \times \boldsymbol{r} \tag{3}$$

here $\boldsymbol{r}$ is the position vector from the rotation axis, which happens to be the radial distance from the cylinder center for the present case. The subscripts *in* and *ro* represent the inertial and rotational frames, respectively. The acceleration in the different frames of reference can be related as follows,

$$\begin{aligned}[D\boldsymbol{v}_{in}/Dt]_{in} &= [D\boldsymbol{v}_{in}/Dt]_{ro} + \boldsymbol{\omega} \times \boldsymbol{v}_{in} \\ &= [D(\boldsymbol{v}_{ro} + \boldsymbol{\omega} \times \boldsymbol{r})/Dt]_{ro} + \boldsymbol{\omega} \times (\boldsymbol{v}_{ro} + \boldsymbol{\omega} \times \boldsymbol{r}) \\ &= [D\boldsymbol{v}_{ro}/Dt]_{ro} + 2\boldsymbol{\omega} \times \boldsymbol{v}_{ro} + \boldsymbol{\omega} \times (\boldsymbol{\omega} \times \boldsymbol{r}) \end{aligned} \tag{4}$$

since,

$$\begin{aligned} \nabla^2 \boldsymbol{v}_{in} &= \nabla^2(\boldsymbol{v}_{ro} + \boldsymbol{\omega} \times \boldsymbol{r}) = \nabla^2 \boldsymbol{v}_{ro} \\ \nabla \boldsymbol{v}_{in} &= \nabla(\boldsymbol{v}_{ro} + \boldsymbol{\omega} \times \boldsymbol{r}) = \nabla \boldsymbol{v}_{ro} \\ \boldsymbol{\omega} \times (\boldsymbol{\omega} \times \boldsymbol{r}) &= -\Omega^2 \boldsymbol{r} \end{aligned} \tag{5}$$

the energy and continuity equations in the rotational frame of reference retain the same form as those in the inertial frame, while the momentum equations contain additional terms such as the centrifugal acceleration represented by $\boldsymbol{\omega} \times (\boldsymbol{\omega} \times \boldsymbol{r})$ in Eq. 4, and the Coriolis acceleration represented by $2\boldsymbol{\omega} \times \boldsymbol{v}_{ro}$ in Eq. 4. By invoking the Boussinesq approximation and the assumption of constant physical properties, one can write the following nondimensionalized governing equations:

$$\nabla \cdot \bar{v}_{ro} = 0 \tag{6}$$

$$D\bar{T}/D\bar{t} = \nu/(Pru_R L)\nabla^2 \bar{T} \tag{7}$$

$$\begin{aligned} D\bar{v}_{ro}/D\bar{t} + 2\Omega L/u_R \boldsymbol{k} \times \bar{v}_{ro} - \Omega^2 L^2/u_R^2 (T_H - T_C)\bar{T}\bar{r} \\ = -\nabla \bar{p} + \nu/(u_R L)\nabla^2 \bar{v}_{ro} - Gr/(u_R L/\nu)^2 \bar{T}\boldsymbol{g}/|g| \end{aligned} \tag{8}$$

where, $\boldsymbol{k}$ is the unit vector in the direction of rotation and $\boldsymbol{\omega} = \Omega\boldsymbol{k}$; u_R is the reference velocity which may take different scales depending on the physical situation. The following scales are used for nondimensionalization: L for length; L/u_R for time; while the pressure and temperature are nondimensionalized by:

$$\bar{T} = (T - T_C)/(T_H - T_C) \tag{9}$$

$$\bar{p} = (p - p_s - \rho\Omega^2 r)/(\rho u_R^2) \tag{10}$$

and the Prandtl and Grashof numbers are given by:

$$Pr = \nu/\alpha, \quad Gr = \frac{g\beta(T_H - T_C)L^3}{\nu^2}$$

In Eq. 8 $\boldsymbol{g}$ is the instantaneous gravitational acceleration vector in the rotational frame of reference, while p_s in Eq. 10 is the static pressure.

When the rotational speed is very low, the buoyancy force becomes dominant so that the scale for the reference velocity is

$$u_R = \nu/L \tag{11}$$

the governing Eqs. 6–8 then become,

$$\nabla \cdot \bar{v}_{ro} = 0 \tag{12}$$

$$D\bar{T}/D\bar{t} = 1/Pr\nabla^2 \bar{T} \tag{13}$$

$$\begin{aligned} D\bar{v}_{ro}/D\bar{t} + 2Re\boldsymbol{k} \times \bar{v}_{ro} - Gr_{ro}\bar{T}\bar{r} \\ = -\nabla \bar{p} + \nabla^2 \bar{v}_{ro} - Gr\bar{T}\boldsymbol{g}/|g| \end{aligned} \tag{14}$$

where Re is the rotational Reynolds number and Gr_{ro} is rotational Grashof number, and they are defined as

$$Re = \Omega L^2/\nu, \quad Gr_{ro} = \beta\Omega^2(T_H - T_C)L^4/\nu^2$$

It is seen from Eq. 14 that at low rotational speed, the centrifugal and Coriolis forces (Re and Gr_{ro}) are much smaller compared to the buoyancy force, so that they can be neglected. Then Eq. 14 and the nonslip boundary conditions return to those in the inertial frame of reference without rotation, except that $\boldsymbol{g}$ is a function of the rotational speed and time with components in the

radial and azimuthal directions of the cylinder, Figure 1, given by

$$g_r = -g \sin \Theta_{ro} = -g \sin (\Theta_0 + \Omega t) \tag{15}$$

$$g_\theta = -g \cos \Theta_{ro} = -g \cos (\Theta_0 + \Omega t) \tag{16}$$

It appears that the system is in a quasisteady state in the sense that all dependent variables solved for a stationary cylinder can be applied to the slow rotational-speed case by simply replacing Θ_{ro} by $\Theta_0 + \Omega t$. The heat transfer rate through the end surfaces at point (r, Θ_{ro}) will simply be,

$$\begin{aligned} Nu_{ro} &= Nu_{ro}(r, \Theta_{ro}, t) \\ &= Nu_{in}(r, \Theta_0 + \Omega t) \end{aligned} \tag{17}$$

where Θ_0 is the angular position at $t = 0$. The long time solution of Eq. 14 is periodical so that the average heat transfer rate with respect to time is

$$Nu(r) = (1/2\pi) \int_0^{2\pi} Nu_{in}(r, \Theta_{in}) d\Theta_{in} \tag{18}$$

It can be seen that, at low rotational speeds, the nonuniform heat transfer on the end surfaces, which is due to natural convection in a stationary cylinder, is averaged along the circumference over time, so that the heat transfer depends only on r spatially.

At high rational speeds, the scale for the reference velocity may be taken as,

$$u_R = \Omega L \tag{19}$$

so that the governing equations become,

$$\nabla \cdot \bar{v}_{ro} = 0 \tag{20}$$

$$D\bar{T}/D\bar{t} = 1/(PrRe)\nabla^2 T \tag{21}$$

$$\begin{aligned} D\bar{v}_{ro}/D\bar{t} + 2\boldsymbol{k} \times \bar{v}_{ro} - \beta(T_H - T_C)\bar{T}\bar{r} \\ = -\nabla p + 1/Re\nabla^2 \bar{v}_{ro} - Gr/Re^2 \bar{T}\boldsymbol{g}/|g| \end{aligned} \tag{22}$$

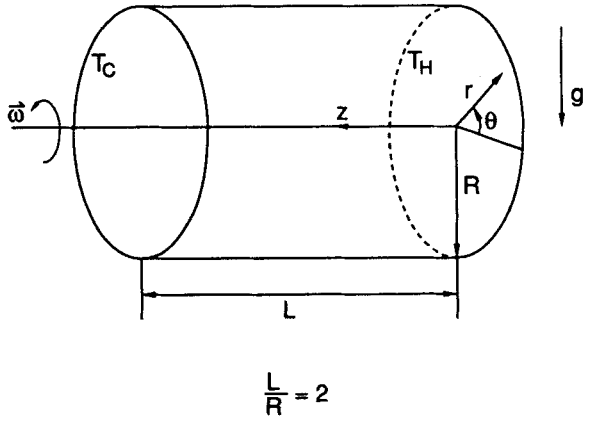

Figure 1. Rotating horizontal cylinder.

From Eq. 22, we see that when the rotational speed is increased, the buoyancy term represented by $Gr/Re^2Tg/|g|$ becomes less important, and the centrifugal and Coriolis forces begin to play a role. When the rotational speed is sufficiently high, the buoyancy term becomes vanishingly small, due to both dominant rotation ($Gr/Re^2 \ll 1.0$) and the rapid variation of gravitational vector g with time (Eq. 22). For this case, the boundary layer characteristics of natural convection also vanish and a trivial solution of Eq. 20–22 is simply the rest state relative to the rotational frame of reference (Greenspan, 1968), or a rigid body motion, where the centrifugal force is balanced by the pressure gradient. This is the case where the heat transfer rate reduces to that of pure conduction, i.e., $Nu = 1.0$.

Numerical Calculations and Results

Numerical calculations have been carried out for a fixed Grashof number of 1.43×10^6, with Gr/Re^2 varied from 7.0×10^{-2} to ∞. This covers the entire range from natural convection-dominant flow to rotation-dominant flow. The numerical solution procedure is the one developed for governing equations in the three-dimensional general orthogonal coordinates, which can be applied directly to the cylindrical geometry. The governing equations are in the primitive variable form, a control volume finite difference is applied to discretize the conservation equations. The convection terms are approximated by the QUICK scheme which is originally developed by Leonard (1983), and the diffusion terms are by central differences. The pressure correction and the solution procedure follow that suggested by Patankar (1980). The grids are nonuniformly distributed to resolve the boundary layer behaviors near the wall regions. The detailed derivations of the equations, discretizations, and grid-refinement studies have been described by Yang et al. (1988) and will not be repeated here. It is to be pointed out that the governing equations in the inertial frame of reference are solved here, so that boundary conditions 1 and 2 are used, in contrast to Eqs. 12–14 or 20–22.

Flow and Temperature Fields in Lateral Planes

The pure natural convection inside a horizontal cylinder with differentially-heated ends have been studied by Yang et al. (1988) at relatively high Rayleigh numbers, and a fixed aspect ratio of $L/R = 2.0$. The flow and temperature fields near the cold wall in the lateral plane at $z = 0.96L$ with the present problem are plotted in Figure 2 at selected Gr/Re^2 numbers. Figure 2a shows the cases without rotation. As the fluid is cooled near the cold end wall, the buoyancy drives the fluid downward and forms a stratified temperature field in the lateral plane. At small rotational speed with $Gr/Re^2 = 7.13$ (Figure 2b), the velocity field is almost unchanged compared to that in the stationary-cylinder case, except near the cylinder wall where due to rotation, the symmetry with respect to the vertical central line disappears, while the stratified temperature field is tilted with respect to the vertical gravitational vector due to the Coriolis acceleration. Since v_{ro} is mainly along the vertical direction, the Coriolis force is (according to $-\rho \boldsymbol{k} \times v_{ro}$) along the horizontal direction. The combination of the vertical gravity force and the horizontal Coriolis force produces the tilt of the temperature stratification field. With increasing rotational speed, the Coriolis force becomes more important, so that the tilt in the stratification

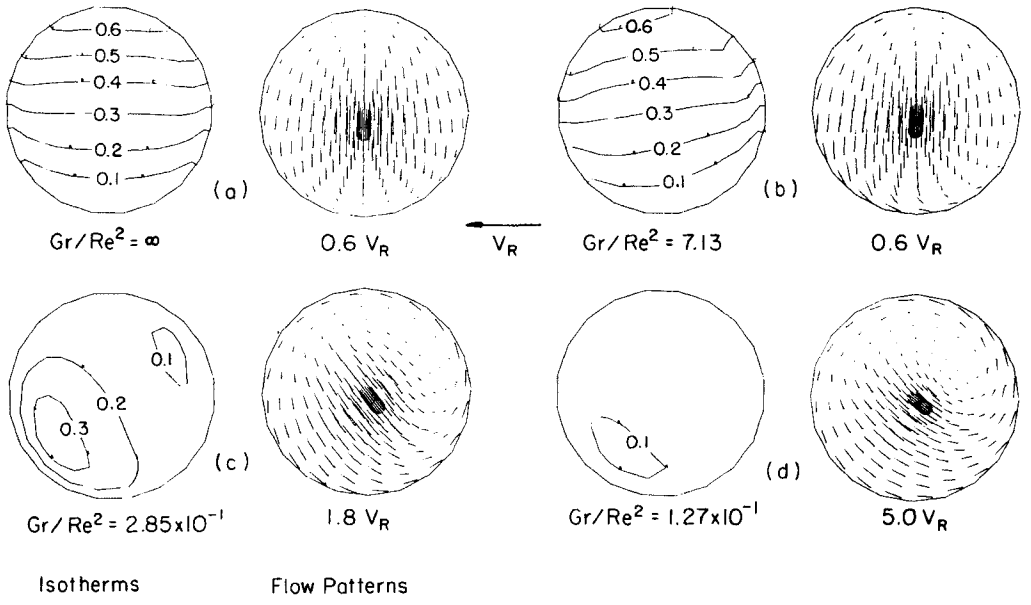

Figure 2. Temperature and velocity fields at $z = 0.96L$ plane.

field is even more pronounced as shown in Figure 2c where Gr/Re^2 is 0.285. As Re^2 is much higher than Grashof number Gr (Figure 2d), the rotational effect overwhelms the natural convection, and the stratified temperature field changes its characteristics and becomes more uniform, while the flow field becomes helical.

Away from the end wall, the flow in the lateral plane consists of four symmetric double helical cells in the upper and lower halves of the cylinder (Kimura and Bejan, 1980; Yang et al., 1988) in the case of a stationary cylinder, Figure 3a. This helical circulation is secondary in the sense that the velocity magnitude is much smaller than the primary circulation, while the temperature field also displays a stratified characteristic. These secondary cells are due to the deformation of the stratified temperature field near the cylindrical wall. However, once the cylinder is being rotated, only two helical cells, which have the same rotational sense as the cylinder itself, survive. Differing from the one near the end wall, the deformation of the temperature stratification field with respect to the vertical gravity happens only near the circular wall boundary, Figures 3b and 3c. This is basically due to the almost stagnant flow in the core with small v_{ro} and small Coriolis acceleration. As the rotational speed increases further, the flow behaves as a rigid body rotation with $v_\theta = r\Omega$ and the temperature field becomes more uniform, Figure 3d.

Flow and Temperature Fields in Vertical Central Plane

The motion in the vertical central plane is mainly buoyancy-driven. In a stationary cylinder, Fig 4a, both thermal and velocity fields show boundary layer characteristics, in that the

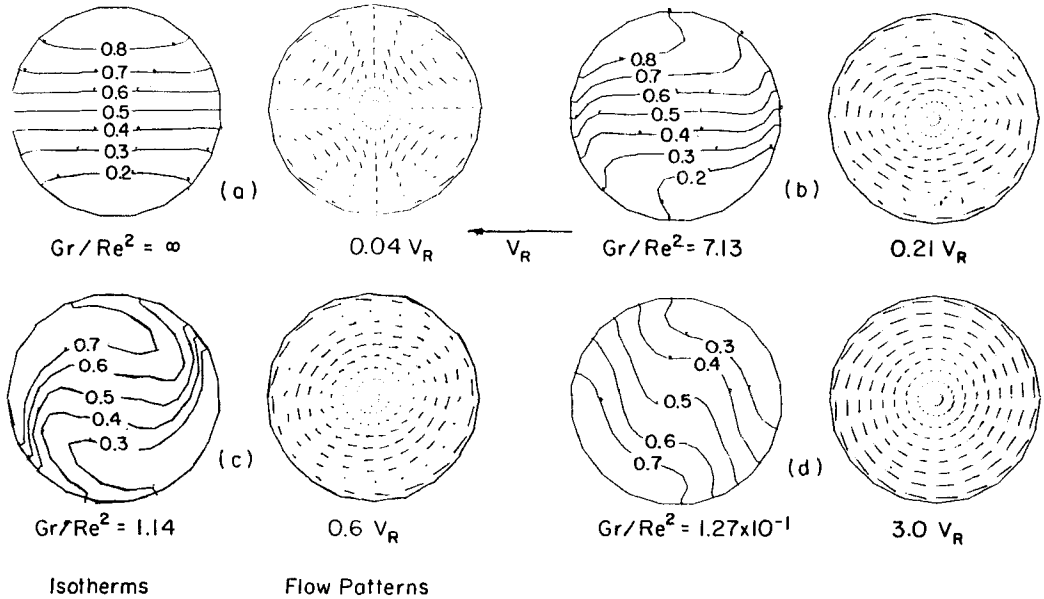

Figure 3. Temperature and velocity fields at central axial plane.

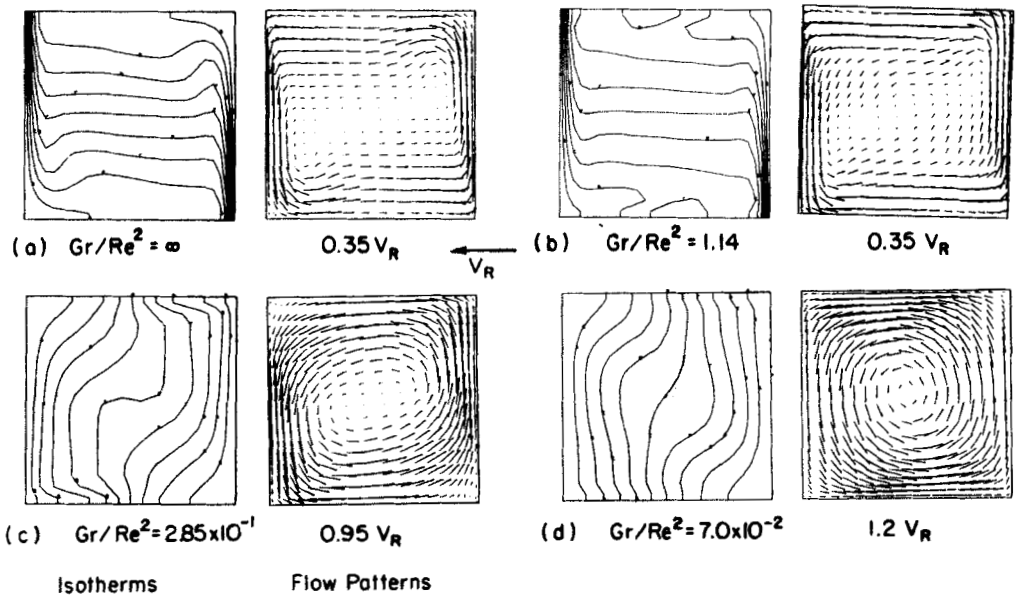

Figure 4. Temperature and velocity fields at vertical central plane.

isotherms are densely distributed near the wall and the temperatures are stratified in the core, and the flows are mainly in the wall region with a stagnant core. At small rotational speeds, the boundary layer characteristics remain, but with some initiation of core motion as seen from the flow patterns in Figure 4b. The isotherms in this case also become less densely packed. Once rotation starts to be important, as in the case for $Gr/Re^2 = 0.285$, Figure 4c, the boundary layer characteristics are totally lost, and the strength of motion is also reduced. Temperature stratification is now nonexistent. These behaviors persist at higher rotational speeds, Figure 4d. From the isotherms, it can be seen that the nonuniformity in heat transfer tends to disappear, but its level is reduced. This is largely due to the time variation of the gravity vector.

Heat Transfer Rates over End Wall Surface

The main objective here is to examine the heat transfer rates over the end surfaces, by means of Nusselt number contours. Shown in Figure 5a is the one on the cold wall in a stationary cylinder. Due to the direct impingement of the hot fluid on the upper portion of the cold surface, a relatively high Nusselt number appears. As the fluid descends along the cold wall due to the buoyancy force, it is cooled down so that the heat transfer rate decreases, thus forming a vertical gradient in Nusselt number. Figure 5b displays the corresponding Nusselt number distribution when $Gr/Re^2 = 7.13$. Similar to isotherms near the cold wall at slower rotational speeds, they exhibit a tilt in the gradient, and this is even more pronounced at higher rotational speeds. When $Gr/Re^2 = 0.285$, the gradients are totally destroyed with relatively uniform variations in heat transfer. Finally, the heat transfer is both uniform and at a lower level.

It is interesting to examine the time-averaged Nusselt number over the circumference, and the local Nusselt number at $r = (\frac{1}{2})R$ at different rotational speeds. $Nu(r)$ is shown in Figure 6. The heat transfer rate over the radial direction exhibits a uniform variation at lower rotational speeds. However, its variation with time is large, Figure 7. At $Gr/Re^2 > 1.1$ it shows a regular periodic variation with time with a maximum value three times higher than the minimum one (at $r = \frac{1}{2}R$). This periodic variation is from the stratification effects. At high rotational speeds for $Gr/Re^2 < 0.28$, the variation in heat transfer is uniform both in time and space.

Figure 8 shows the overall Nusselt number through the end surfaces. If a crystal growth process takes place in a long time, a lower rotational speed is suited in that it can give a higher as well

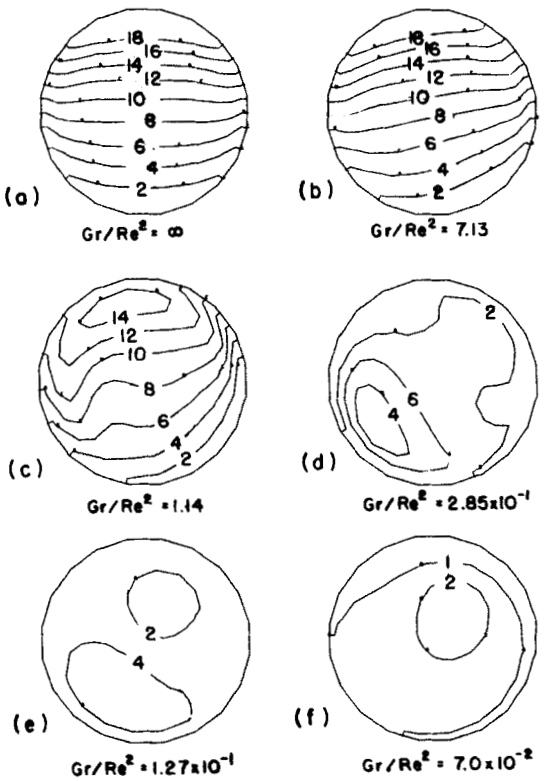

Figure 5. Isopleths of Nusselt numbers at different rotational speeds.

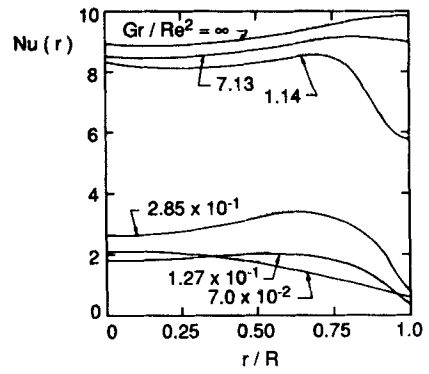

Figure 6. *Nu(r)* at different rotational speeds.

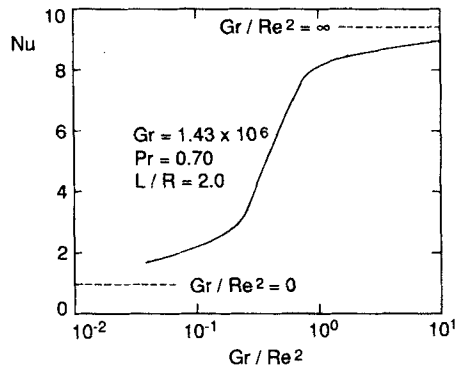

Figure 8. Overall Nusselt number with rotational speeds.

as more uniform transfer rate in terms of time average. However, a uniform heat transfer both in time and in space can be reached only at high rotational speed. In general, if the reaction time is given, it is required that

$$\Omega \gg 1/t_{\text{reaction}} \tag{23}$$

to insure proper distribution over the time, while a parameter range

$$Gr/Re^2 > 1.0 \tag{24}$$

will give a fast reaction rate. Equation 24 means that,

$$\Omega < \Omega_{\text{critical}} \tag{25}$$

Here Ω_{critical} is the rotational speed that results in $Gr/Re^2 = 1.0$. By a proper combination of Eqs. 23 and 25, one can have a desired crystal quality. If no Ω exists for Eqs. 23 and 25, one can always change Gr to satisfy the conditions.

Conclusions

Rotational effects on the natural convection in a horizontal cylinder has been studied numerically. The Grashof number is fixed at 1.43×10^6, and the aspect ratio (L/R) is 2.0. The rotational effect is examined with the parameter of Gr/Re^2 ranging from 7.0×10^{-2} to ∞, which cover the rotation dominant to natural convection dominant regions. At low rotational speeds, the rotation tilts the stratified temperature fields in the lateral planes as a result of the Coriolis force. With increasing effects of rotation, temperature becomes more uniform in space, and the strength of the flow due to buoyancy in the vertical plane reduces. At sufficiently high rotational speed, the flow acts like a rigid body.

At small rotational speeds, the effect of rotation is to render the spatial heat flux distribution more uniform. At high rotational speeds, the heat transfer distribution on the end surface is more homogenized but the heat transfer rate is at a lower level due to reduced buoyancy driving force. In an appropriate parameter range one can have both relatively high and uniform heat transfer over the end surfaces.

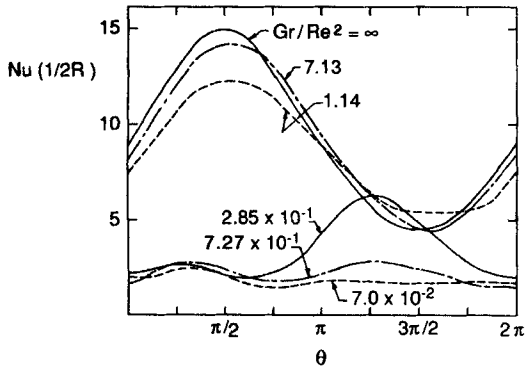

Figure 7. Cyclic variation of *Nu*(½*R*).

Acknowledgment

The authors would like to acknowledge the support of the National Science Foundation under Grant CBT82-19158 to the University of Notre Dame and the Computing Center of the University of Notre Dame.

Notation

g = gravitational acceleration vector
Gr = Grashof number, $g\beta(T_H - T_C)L^3/\nu^2 R$
k = unit vector in the axial direction (also the direction of rotation)
L = length of the cylinder
Nu = Nusselt number
ps = static pressure
p = pressure
Pr = Prandtl number
r = radial coordinate
R = radius of the cylinder
Ra = Rayleigh number, $Gr \cdot Pr$
Re = Reynolds number
t = time
T = temperature
u_R = reference velocity
v = velocity
z = axial coordinate

Greek letters

α = thermal diffusivity
β = volume expansion coefficient
Ω = rotational angular velocity
ω = rotational vector
ν = kinematic viscosity
ρ = density
Θ = angular coordinate
∇ = gradient symbol

Superscript

$-$ = dimensionless quantities

Subscripts

C = cold wall
H = hot wall
in = in the inertial frame of reference
r = in the r direction
ro = in the rotational frame of reference
t = time derivative
0 = initial quantities
Θ = in the Θ direction

Literature Cited

Greenspan, H. P., *The Theory of Rotating Fluids,* Cambridge Univ. Press (1968).

Hamady, F., "Experimental Study of Local Natural Convection Heat Transfer in Inclined and Rotating Enclosures," Ph.D. Thesis, Michigan State Univ. (1987).

Hessami, M. A., G. De Vahl Davis, E. Leonardi, and J. A. Reizes, "Mixed Convection in Vertical, Cylindrical Annuli," *Int. J. Heat Mass Transf.,* **30,** 151 (1987).

Kimura, K., and A. Bejan, "Numerical Study of Natural Circulation in a Horizontal Duct with Different End-Temperatures," *Warme-Und Stoffubertragung,* **14,** 269 (1980).

Leonard, B. P., "A Convective Stable, Third-Order Accurate Finite-Difference Method for Steady Two-Dimensional Flow and Heat Transfer," *Numerical Properties and Methodologies in Heat Transfer,* T. M. Shih, ed., Hemisphere, Washington, DC, 211 (1983).

Markham, B. L., and F. Rosenberger, "Diffusive-Convective Vapor Transport Across Horizontal and Inclined Rectangular Enclosures," *J. of Crystal Growth,* **67,** 241 (1983).

Mughal, S. A., and B. Ray, "Preparation and Crystallization of ZnSiP2 by the Iodine Vapor Transport Method," *J. of Cry. Growth,* **21,** 146 (1974).

Ostrach, S., "Fluid Mechanics in Crystal Growth—The 1982 Freeman Scholar Lecturer," *J. Fluid Eng.,* **105,** 5 (1983).

Patankar, S. V., *Numerical Heat Transfer and Fluid Flow,* Hemisphere, Washington, DC (1980).

Randriamampiania, A., P. Bontoux, and B. Roux, "Buoyancy Driven Flows in Rotating Cylindrical Annulus," *Int. J. Heat Mass Transf.,* **30,** 1275 (1987).

Ranganathan, P., and R. Viskanta, "Natural Convection of Binary Gas in Rectangular Cavities" *Proc. of ASME/JSME Therm. Eng. Joint Conf.,* **3,** 293 (1987).

Rosenberger, F., "Fluid Dynamics in Crystal Growth from Vapors," *Phys-Chem. Hydrodyn.,* **1,** 3 (1979).

Schiroky, G. H., and F. Rosenberger, "Free Convection of Gases in a Horizontal Cylinder with Differentially Heated End Walls," *Int. J. Heat Mass Transf.,* **27,** 587 (1984).

Smutek, C., P. Bontoux, B. Roux, G. H. Schiroky, A. C. Hurford, F. Rosenberger, and G. De Vahl Davis, "Three Dimensional Convection in Horizontal Cylinders: Numerical Solutions and Comparison with Experimental and Analytical Results," *Numer. Heat Transf.,* **8,** 613 (1985).

Solan, A., and S. Ostrach, "Convection Effects in Crystal Growth by Closed-tube Chemical Vapor Transport," *Preparation and Properties of Solid State Materials,* W. R. Wilcox, ed., Marcel Dekker, **4,** 63 (1976).

Yang, H. Q., K. T. Yang, and J. R. Lloyd, "A Numerical Study of Three-Dimensional Laminar Natural Convection in a Horizontal Cylinder with Differentially-heated End Walls at High Rayleigh Numbers," *Numer. Heat Transf.,* in press (1988).

Manuscript received Dec. 23, 1987, and revision received May 2, 1988.